

The Influence of Extreme Levels of the Solar Wind Dynamic Pressure on the Structure of Nightside Auroral Precipitation

V. G. Vorobjev^{a, *}, O. I. Yagodkina^{a, **}, E. E. Antonova^{b, c, ***}, and I. P. Kirpichev^{c, ****}

^a Polar Geophysical Institute, Apatity, Murmansk oblast, Russia

^b Skobel'syn Institute of Nuclear Physics, Moscow State University, Moscow, Russia

^c Space Research Institute, Russian Academy of Sciences, Moscow, Russia

*e-mail: vorobjev@pgia.ru

**e-mail: oksana41@mail.ru

***e-mail: elizaveta.antonova@gmail.com

****e-mail: ikir@iki.rssi.ru

Received April 6, 2022; revised July 1, 2022; accepted July 20, 2022

Abstract—The data from the DMSP spacecraft were used to study the characteristics of ion and electron precipitation in the nightside sector of the auroral zone during magnetically quiet periods at extreme values of the solar wind dynamic pressure (P_{sw}). It was shown that the ion pressure at the isotropy boundary (IB) increases with P_{sw} and can reach a level of 4–6 nPa at $P_{sw} = 20$ –22 nPa. The latitude profiles of the ion pressure obtained at different levels of P_{sw} indicate that the increase in P_{sw} is accompanied by an expansion of the ion precipitation region and a shift of the IB to lower latitudes. At $\langle P_{sw} \rangle = 0.5$ nPa, the IB latitude is $\sim 70.4^\circ$ CGL, while at $\langle P_{sw} \rangle = 16.3$ nPa, it shifts toward the equator to $\sim 64.6^\circ$ CGL. As the P_{sw} level decreases, the energy fluxes of precipitating electrons decrease significantly. At $P_{sw} < \sim 2.0$ nPa, auroras in the region of the auroral oval can be considered subvisual. At extremely low values of dynamic pressure, $P_{sw} = \sim 0.2$ nPa, it becomes very problematic to identify the zone of electron and ion precipitation.

DOI: 10.1134/S0016793222060160

1. INTRODUCTION

Isotropization of the pitch-angle distribution of energetic particles takes place in the equatorial plane of the magnetosphere mainly due to a change in the curvature radius of magnetic field lines with distance from the Earth (Sergeev et al., 1993). The radial distance at which isotropization occurs depends on the particle energy: the lower the energy is, the further from the Earth, on average, isotropization occurs. In the region of isotropic plasma, its properties remain constant along the geomagnetic field line, which makes possible to determine the characteristics of the magnetospheric plasma from observations of precipitating particles at ionospheric heights. Newell et al. (1996) used the data of low-orbit DMSP spacecraft to identify a boundary, called the b2i boundary, at which the energy flux of precipitating ions reaches a maximum. It was statistically shown (Newell et al., 1998) that the b2i position adequately matches the isotropy boundary (IB) of ions with an energy of 30 keV.

Plasma pressure is one of the most important parameters of the magnetosphere. Under conditions of magnetostatic equilibrium, the plasma pressure largely determines the distribution of field-aligned currents and the stability of magnetospheric plasma

domains. The average distribution of plasma pressure in the plasma ring around the Earth at geocentric distances from 6 to 10 Re was obtained from the THEMIS satellite data (Kirpichev and Antonova, 2011; Antonova et al., 2014). Tsyganenko and Mukai (2003) used the observations of the GEOTAIL satellite at distances from 10 to 50 Re in the nightside magnetosphere to create a 2D model of the plasma pressure distribution. The results of that study indicate a significant increase in the plasma pressure in the equatorial plane of the magnetosphere with an increase in the solar wind dynamic pressure (P_{sw}). The ion pressure in the nightside sector of the auroral zone at the b2i boundary and its dependence on P_{sw} was studied by Vorobjev et al. (2019) from the DMSP satellite data, and a linear relationship between these parameters was found.

The results of the studies cited above were obtained by processing large arrays, in which statistically significant datasets on the solar wind dynamic pressure were presented mainly in the P_{sw} range from 1.0 to 6.0 nPa. The aim of this study is to examine the structure of ion and electron precipitation and determine the features of the latitudinal distribution of precipitating auroral particles and the magnitude of the ion pressure at the IB at extreme values of the solar wind dynamic pres-

sure. Extreme values of the dynamic pressure are understood as $P_{sw} < 1.0$ nPa and $P_{sw} > 6.0$ nPa. Such P_{sw} values are beyond the scope of commonly used databases and are only possible as a result of the analysis of individual events specially selected for this purpose.

2. THE DATA

The study used the data from the DMSP F6 and F7 spacecraft for the full year of 1986 and the data from the same series of spacecrafts for individual, specially selected periods. The spacecraft of the DMSP series recorded the spectra of precipitating ions and electrons every second in the energy range from 30 eV to 30 keV. The corrected geomagnetic coordinates (CGL, MLT) of the satellite trajectory at an altitude of 110 km were calculated using the AACGM model (Baker and Wing, 1989).

The method for determining ion pressure from the DMSP satellite measurements was first published by Wing and Newell (1998). In our study, we used a modified version of that method, which was proposed by Stepanova et al. (2006). The ion pressure is calculated under the assumption of a Maxwellian energy distribution of particles, which, despite the recorded non Maxwellian energetic tails of the distribution functions, does not lead to significant errors in calculating the pressure in the considered regions (Kirpichev et al., 2021). To avoid a significant effect of substorm processes on the results of the study, an important criterion in selecting the data and study intervals was the low level of magnetic activity in the auroral zone, $AL > -200$ nT.

To study the effect of extremely high P_{sw} levels on the ion pressure, we selected magnetic storms for which large P_{sw} values were observed before the onset of the main phase at positive Dst index. Such intervals are classically referred to as DCF phases (disturbance of corpuscular flux) of magnetic storms. Under the condition of a low level of magnetic activity in the auroral zone, such intervals corresponded to the DCF phases of magnetic storms on June 13–14, 1998, April 16–17, 1999, March 18–19, 2002, November 19–20, 2007, and May 31, 2013. Magnetic storms on May 31, 2013 and March 18, 2002 were preceded by magnetically quiet periods lasting more than 24 h, which were used to study the latitudinal distribution of precipitating particle characteristics at low and extremely low P_{sw} values.

To analyze the variations in the geomagnetic activity indices and parameters of the interplanetary medium, we used the data presented at <http://wdc.kugi.kyoto-u.ac.jp/> and <http://cdaweb.gsfc.nasa.gov/>.

3. THE EFFECT OF P_{sw} ON THE ION PRESSURE

The ion energy fluxes (J_i) and their average energies (E_i) in the nightside sector of the auroral zone gradually increase with decreasing latitude, reaching a

maximum at the equatorial edge of precipitation. According to Newell et al. (1996), the position of the J_i maximum was determined as the isotropy boundary. Equatorward from the IB, the energy fluxes of the precipitating ions rapidly decrease. Thus, the IB determines the position of the ion pressure maximum, and its latitude determines the most equatorial region of the ionosphere, the ion pressure in which can be projected into the equatorial magnetosphere.

Due to the characteristics of the trajectories of the DMSP spacecraft, the maximum number of satellite passages across the auroral precipitation region during the events under study was located in the 1800–2100 MLT sector. Figure 1a shows the dependence of the ion pressure at the IB on the solar wind dynamic pressure in this MLT sector (line 1) based on the statistical data set for 1986. Since the isotropy boundary is not an isobar, the magnitude of the ion pressure at the IB depends on the MLT. For comparison, Fig. 1a (line 2) shows similar data in the 2100–2400 MLT sector (Vorobjev et al., 2019). The figure shows that the ion pressure at the IB in the 2100–2400 MLT sector is slightly higher than the pressure in the 1800–2100 MLT sector. This is clearly shown by the vertical dashed line drawn at the level $P_{sw} = 6$ nPa, at which the ion pressure is ~ 1.0 nPa in the 1800–2100 MLT sector and ~ 1.3 nPa in the 2100–2400 MLT sector. The standard deviation of the data in Fig. 1a is ~ 0.2 – 0.3 nPa, and it is discussed in more detail by Vorobjev et al. (2019).

Figure 1b shows the ion pressure at the IB in the 1800–2100 MLT sector using data for the periods of the DCF phase of the magnetic storms we selected. The solid line near the origin of the coordinates corresponds to the data shown in Fig. 1a, line 1. The dashed line corresponds to the linear regression equation obtained for all points on the graph (linear correlation coefficient $r = 0.82$). The scatter of the points is significant, but there is an obvious nearly linear growth of the ion pressure with increasing P_{sw} . A separate point on the graph at $P_{sw} = 19.3$ nPa indicates that the ion pressure at the IB can reach ~ 10 nPa.

4. THE LATITUDE PROFILES OF AURORAL PRECIPITATION CHARACTERISTICS AT DIFFERENT P_{sw} LEVELS

The solar wind dynamic pressure under quiet conditions usually does not exceed ~ 3 nPa. For example, in the paper by Tsyganenko and Mukai (2003), the average $P_{sw} \sim 2.2$ nPa, and according to the data for 1986, it is about 2.4 nPa. A sharp surge in the solar wind dynamic pressure was observed in the event of March 18, 2002; it was recorded as SSC at 1322 UT, after which the solar wind dynamic pressure remained very high for ~ 10 h, varying in the range of 14–20 nPa. The DMSP satellite data for this period were used to determine the latitudinal distribution of the ion pressure and energy fluxes of precipitating electrons at extremely high P_{sw} levels. Figure 2 (top panel) shows

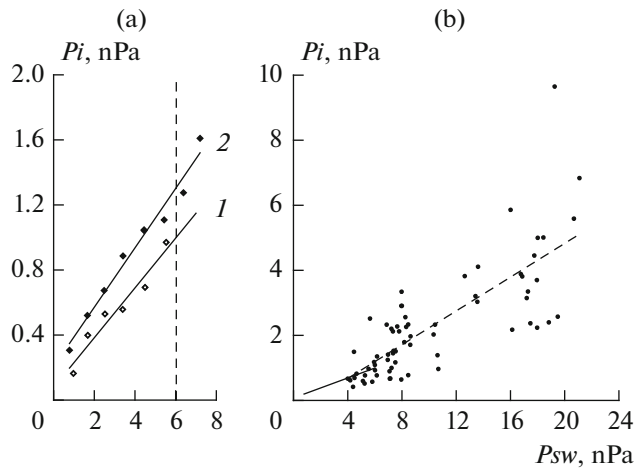


Fig. 1. (a) The ion pressure at the isotropy boundary (IB) as a function of the solar wind dynamic pressure, P_{sw} : (1) in the 1800–2100 MLT sector, (2) in the 2100–2400 MLT sector. (b) Ion pressure at the IB in the 1800–2100 MLT sector during periods of extremely large P_{sw} values.

the latitudinal ion pressure profile obtained by averaging over 10 DMSP satellite passages of the auroral precipitation zone. The horizontal axis in the figure is the corrected geomagnetic latitude (CGL). The averaging was carried out by the method of superposed epochs relative to the isotropy boundary, whose average position was $\langle \Phi' \rangle = 64.6^\circ$ CGL, $\langle \text{MLT} \rangle = 20.4$, $\langle AL \rangle = -44$ nT. At the solar wind dynamic pressure $\langle P_{sw} \rangle = 16.3$ nPa, the ion pressure at the isotropy boundary $\langle P_i \rangle = 5.1$ nPa.

The average latitudinal distribution of electron precipitation energy fluxes (J_e) is shown in the bottom panel of Fig. 2. The maximum J_e values, as in the studies by Yahnin et al. (1997) and Starkov et al. (2005), are observed poleward from the IB in the region of the oval of discrete aurora forms, the width of which is about 2° CGL.

Auroral intensity can be estimated using the method proposed by Vorobjev et al. (2013). In that paper, to calculate the 557.7 nm intensity, the authors took into account the processes of formation of an electron excited O(¹S) atom as a result of the transfer of excitation energy from the metastable state $N_2(A^3\Sigma_u^+)$, excitation of O(³P) by primary and secondary electrons, and dissociative recombination. According to this method, the [OI] 557.7 nm intensity at peak J_e values is about 1.4 kR. The precipitation equatorward to the isotropy boundary are associated with a diffuse glow, the intensity of which rapidly decreases with decreasing latitude.

Prior to the onset of the solar wind disturbances in the event of March 18, 2002, the solar wind dynamic pressure remained at a level of about ~ 2 nPa for a long time. Figure 3 shows the average characteristics of ion

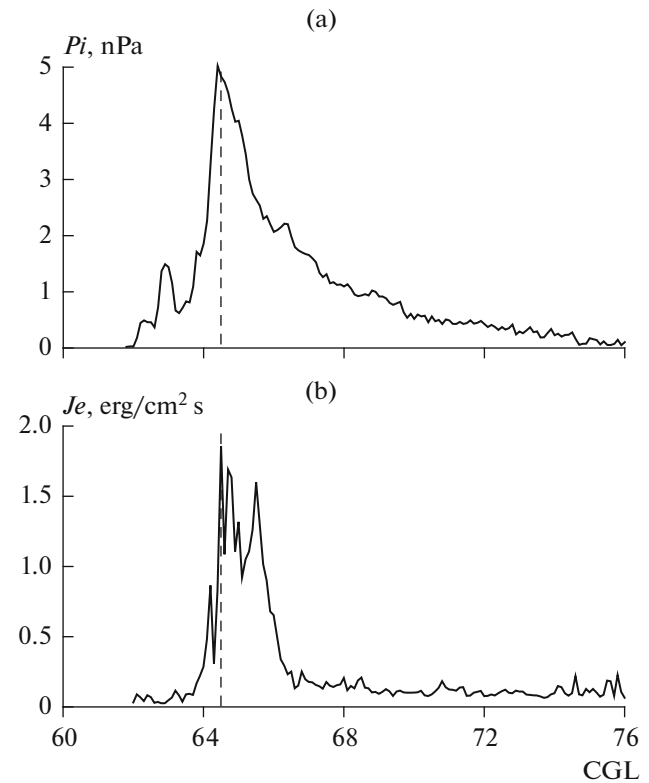


Fig. 2. The average latitude profiles of ion pressure (top panel) and energy fluxes of precipitating electrons (bottom panel) at $\langle P_{sw} \rangle = 16.3$ nPa. The vertical dashed line is the position of the isotropy boundary.

and electron precipitation over this period. The format of the figure is the same as Fig. 2. The top panel shows the average latitudinal distribution of the ion pressure. At an average dynamic pressure $\langle P_{sw} \rangle = 2.1$ nPa, the ion pressure at the IB was $\langle P_i \rangle = 0.7$ nPa; the average position of the IB $\langle \Phi' \rangle = 68.6^\circ$ CGL. Thus, with a decrease in the $\langle P_{sw} \rangle$ level from 16.3 to 2.1 nPa, the isotropy boundary shifted by $\sim 4^\circ$ to the pole, and the level of ion pressure at the IB decreased by a factor of ~ 7 .

As in the case of high P_{sw} levels, the maximum energy fluxes of precipitating electrons are recorded poleward of the IB. The width of the precipitation region of the auroral oval has not changed significantly and is $\sim 2^\circ$ CGL, but the [OI] 557.7 nm emission intensity at the peak J_e values decreased to 0.5 kR. Discrete forms of this intensity belong to very weak visual auroras.

In the quiet period before the onset of the magnetic storm on May 31, 2013, an even lower level of P_{sw} was observed, the value of which was less than 1 nPa. The top panel of Fig. 4 shows the latitudinal variation of the ion pressure for $\langle P_{sw} \rangle = 0.5$ nPa. As compared to the data in Fig. 3, the IB position shifted another $\sim 2^\circ$ poleward to the latitude $\langle \Phi' \rangle = 70.4^\circ$ CGL, and the level of ion pressure at the isotropy boundary decreased to $\langle P_i \rangle = 0.1$ nPa.

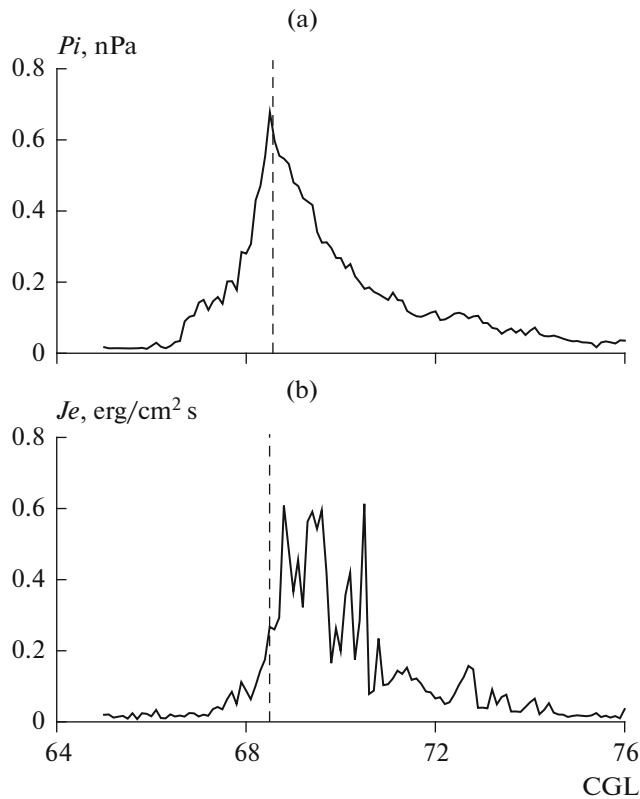


Fig. 3. The same as in Fig. 2 for $\langle P_{sw} \rangle = 2.1$ nPa: the average IB position $\langle \Phi \rangle = 68.6^\circ$ CGL, $\langle \text{MLT} \rangle = 20.0$ at $\langle AL \rangle = -49$ nT.

Same as at higher levels of the solar wind dynamic pressure, the maximum the energy fluxes of precipitating electrons are recorded at the isotropy boundary and poleward from it. The width of the auroral oval precipitation region, as before, is about 2° CGL. The peak values of the [OI] 557.7 nm intensity are estimated at 0.12–0.16 kR, which approximately corresponds to the level of the night sky airglow. Bursts of intensity at latitudes above $\sim 72^\circ$ CGL are related to polar cap precipitation.

The lowest level of solar wind dynamic pressure was observed on May 30, 2013 in the interval 1830–2030 UT. Figure 5 shows the data obtained by satellites F18 at 1951 UT (a) and F17 at 2019 UT (b) in the Southern Hemisphere at $P_{sw} = 0.23$ nPa. The 5-min average values of the AL index were -26 and -29 nT, respectively. The figure shows that under such extremely quiet conditions it becomes very problematic to identify the zone of ion precipitation and determine the position of the isotropy boundary. The ion pressure varies relative to the average level of ~ 0.02 nPa with randomly appearing peak values up to ~ 0.06 nPa. The average Je level is also very low with small-scale enhancements up to 0.2 – 0.4 erg/cm 2 s, which may reflect the presence of weak subvisual forms of auroras.

The comparison of the data presented in Figs. 2–5 reliably demonstrates that the maximum ion pressure

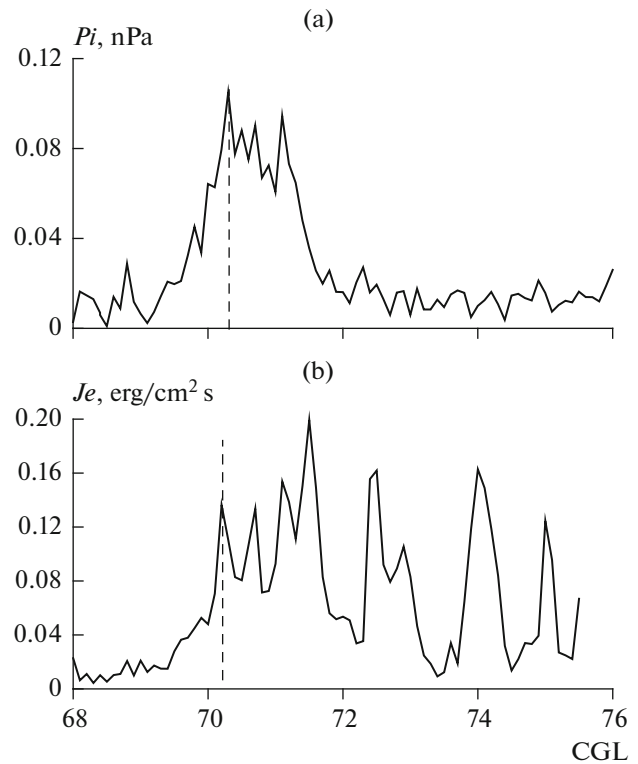


Fig. 4. The same as in Fig. 2 for $\langle P_{sw} \rangle = 0.5$ nPa: the average IB position $\langle \Phi \rangle = 72.2^\circ$ CGL, $\langle \text{MLT} \rangle = 20.4$ at $\langle AL \rangle = -26$ nT.

in the auroral zone, the latitudinal position of the isotropy boundary, and the level of the energy flux of electrons precipitating in the auroral oval depend significantly on the solar wind dynamic pressure. As P_{sw} increases, the ion pressure level increases as well, while the IB shifts to lower latitudes. For example, at $\langle P_{sw} \rangle = 16.3$ nPa, the IB latitude is $\sim 64.6^\circ$ CGL, the ion pressure is $\langle Pi \rangle = 5.1$ nPa; at $\langle P_{sw} \rangle = 0.5$ nPa, the IB latitude is already 70.4° CGL, and $\langle Pi \rangle = 0.1$ nPa.

5. RESULTS AND DISCUSSION

The data from DMSP spacecraft were used to study the characteristics of ion and electron precipitation in the 1800–2100 MLT sector of the auroral zone at extreme values of the solar wind dynamic pressure (P_{sw}). The main results obtained in the study can be formulated as follows:

(1) The ion pressure at the isotropy boundary in the 1800–2100 MLT sector is ~ 0.8 of the ion pressure in the 2100–2400 MLT sector.

(2) At extremely high levels of the solar wind dynamic pressure, the ion pressure at the IB increases with increasing P_{sw} and can reach a level of 4–6 nPa at $P_{sw} = 20$ – 22 nPa.

(3) Latitude profiles of the ion pressure were obtained at average dynamic pressure levels of 0.5, 2.1,

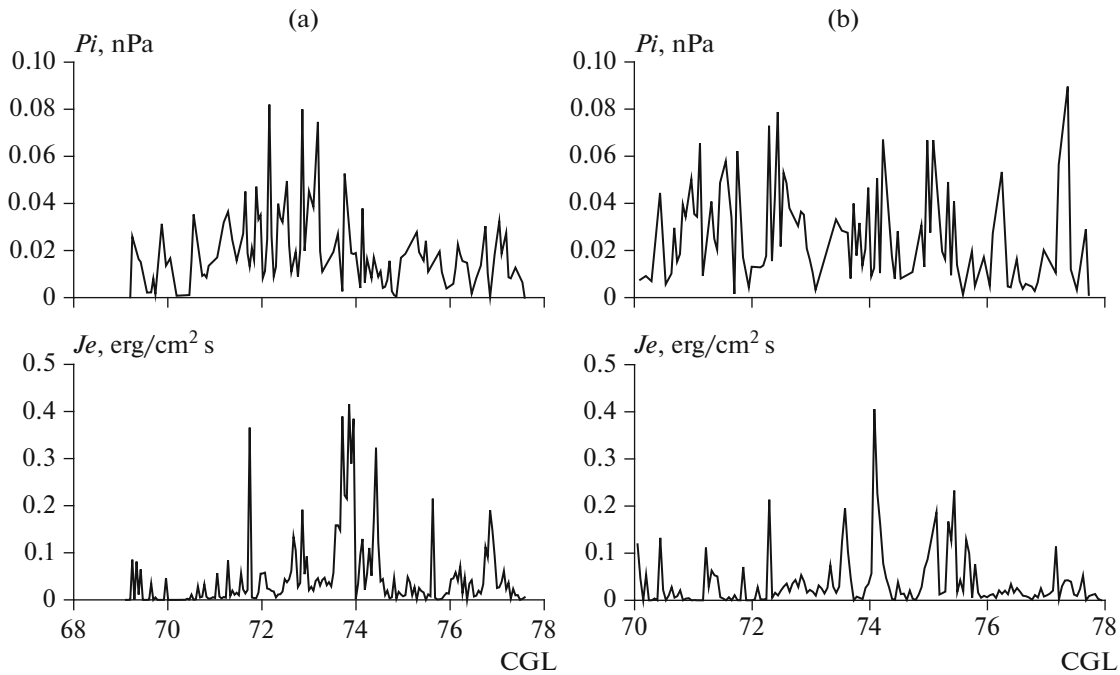


Fig. 5. Observations of the satellites (a) F18 at 1951 UT and (b) F17 at 2019 UT in the Southern Hemisphere at $P_{sw} = 0.23$ nPa.

and 16.3 nPa, indicating that an increase in P_{sw} is accompanied not only by an increase in the plasma pressure in the auroral zone, but also by an expansion of the ion precipitation region, mainly due to the IB shifting to lower latitudes. For example, at $\langle P_{sw} \rangle = 0.5$ nPa, the IB latitude is $\sim 70.4^\circ$ CGL, while at $\langle P_{sw} \rangle = 16.3$ nPa, it is already $\sim 64.6^\circ$ CGL.

(4) With a decrease in the dynamic pressure of the solar wind, the latitudinal dimensions of the auroral oval precipitation region do not change significantly; however, the energy fluxes of precipitating electrons and, therefore, the auroral intensity decrease significantly.

(5) At extremely low values of dynamic pressure, $P_{sw} = \sim 0.23$ nPa, it is not possible to reliably identify the zone of electron and ion precipitation and determine the position of the isotropy boundary.

Roach and Jamnick (1958) noted that the weakest glow that the human eye can discern in the night sky should be 3 or 4 times more intense than the normal night sky airglow. In both the red and green lines of atomic oxygen, the airglow intensity of the clear night sky at high latitudes is ~ 0.15 – 0.20 kR. Thus, at $P_{sw} < \sim 2.0$ nPa, auroras in the region of the auroral oval can be attributed to the subvisual type. However, large small-scale peaks observed in the latitudinal distribution of Je do not exclude the possibility of the occurrence of weak visual forms of auroras in certain periods.

Auroral precipitation at latitudes above the isotropy boundary is considered to be isotropic. In the region of isotropic precipitation under magnetostatic

equilibrium conditions, the plasma pressure is constant along the geomagnetic field line and can be used as a “marker” in determining the pressure in the equatorial plane of the magnetosphere. This method, called the “morphological projection” method, was proposed by Paschmann et al. (2002) and Antonova et al. (2018) and we used it earlier (Antonova et al., 2014; Kirpichev et al., 2016). The method is based on a comparison of the latitudinal distribution of pressure at ionospheric heights with the distribution of plasma pressure in the equatorial plane of the magnetosphere. The ion pressure in the magnetosphere was determined using the THEMIS satellite observations. The radial pressure distribution in the equatorial plane ($Z_{SM} = 0 \pm 1$ Re) on the meridian $MLT = 20 \pm 1$ is shown in Fig. 6a. The pressure profile was obtained for magnetically quiet conditions ($AL > -200$ nT, $Dst > -20$ nT, $P_{sw} = 2.0 \pm 0.2$ nPa), which were identical to the conditions under which the latitude profile of the ionospheric ion pressure was obtained (shown in Fig. 3 for the level $\langle P_{sw} \rangle = 2.1$ nPa).

Figure 6b shows the projection of the latitude profile of the ion pressure onto the equatorial plane of the magnetosphere, provided that the pressures are equal along the geomagnetic field lines. The upper horizontal scale in Fig. 6b shows the corrected geomagnetic latitudes, and the lower one shows the radial distance for which these latitudes are projected. The arrow indicates the position of the isotropy boundary. The figure shows that, under average quiet conditions, the isotropic boundary in the equatorial plane is located at a distance of ~ 7.0 Re. The IB position corresponds to

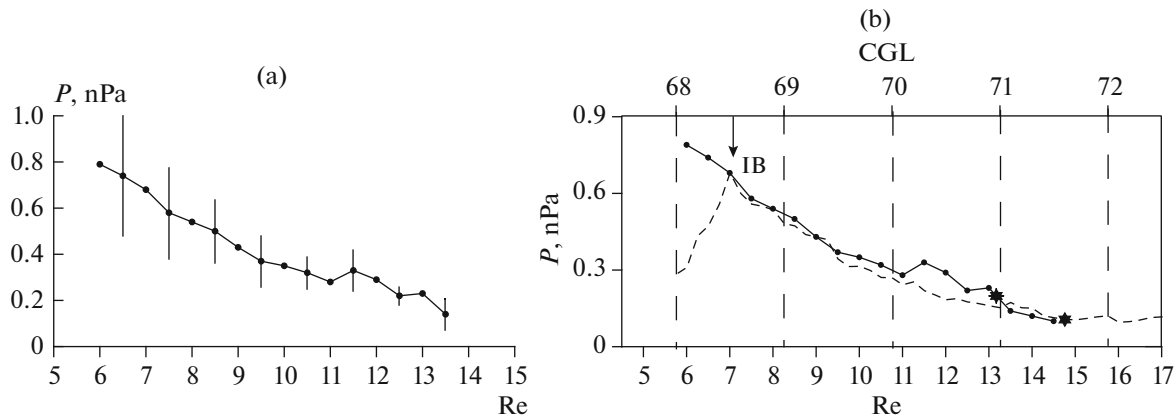


Fig. 6. (a) The radial distribution of ion pressure at the 20 ± 1 MLT meridian; (b) projection of the latitude profile of the ion pressure at $\langle P_{sw} \rangle = 2.1$ nPa onto the equatorial plane of the magnetosphere.

the position of the equatorial boundary of the auroral oval electron precipitation.

The position of the polar boundary of electron precipitation in the equatorial plane in Fig. 6b can be determined in two ways: (1) by the pressure level at this boundary (the asterisk at 13.3 Re) and (2) by the mean latitude of the boundary (the asterisk at 14.8 Re). Thus, the polar boundary of the auroral oval precipitation during magnetically quiet periods at an average solar wind dynamic pressure of ~ 2.0 nPa is located in the equatorial plane at distances of 13–15 Re.

It should also be noted that the occurrence of magnetospheric storms and substorms can lead to a change in the dependence of pressure at the auroral oval latitudes on the dynamic pressure of the solar wind. For example, it was shown (Rojas-Gamarra et al., 2020) using the data from the DMSP spacecraft that the proportionality between the maximum plasma pressure in the auroral oval and the solar wind dynamic pressure is violated with the onset of a substorm.

On the whole, the results obtained in this study indicate that the dynamic pressure of the solar wind under magnetically quiet conditions largely determines the plasma pressure inside the magnetosphere. The pressure determined from the data of low-flying satellites at the latitudes of the auroral oval can be used to analyze the distribution of plasma pressure near the equatorial plane.

6. CONCLUSIONS

The characteristics of ion and electron precipitation in the nightside sector of the auroral zone at the solar wind dynamic pressure (P_{sw}) in the range from ~ 0.2 to ~ 20 nPa were studied using the data from the DMSP spacecraft. It was shown that at extremely high levels of the solar wind dynamic pressure the ion pressure at the isotropy boundary increases with P_{sw} and can reach a level of 4–6 nPa at $P_{sw} = 20$ –22 nPa. The

latitude profiles of the ion pressure obtained at different levels of dynamic pressure indicate that the increase in P_{sw} is accompanied by the expansion of the ion precipitation region and a shift of the IB to lower latitudes. For example, at $\langle P_{sw} \rangle = 0.5$ nPa, the IB latitude is $\sim 70.4^\circ$ CGL, while at $\langle P_{sw} \rangle = 16.3$ nPa it is already $\sim 64.6^\circ$ CGL.

With a decrease in the level of the solar wind dynamic pressure, the energy fluxes of precipitating electrons are significantly reduced and the intensity of the auroral glow decreases accordingly. At $P_{sw} < \sim 2.0$ nPa, auroras in the region of the auroral oval can be attributed to the subvisual type. At extremely low values of dynamic pressure, $P_{sw} = \sim 0.2$ nPa, it becomes very problematic to identify the zone of electron and ion precipitation and determine the position of the isotropy boundary.

The “morphological projection” method was used to project the latitude profile of the ion pressure onto the equatorial plane of the magnetosphere at $\langle P_{sw} \rangle = 2.1$ nPa. It was shown that the isotropy boundary and the equatorial boundary of the electron precipitation of the auroral oval are located in the equatorial plane at a distance of ~ 7.0 Re, while the polar boundary is located at distances of 13–15 Re from the Earth.

ACKNOWLEDGMENTS

The DMSP spacecraft data are taken from the website <http://sd-www.jhuapl.edu>; the IMF and solar wind plasma parameters and magnetic activity indices are taken from the websites <http://wdc.kugi.kyoto-u.ac.jp/> and <http://cdaweb.gsfc.nasa.gov/>.

FUNDING

The study carried out by V.V.G. was supported by the Russian Science Foundation (RSF), project no. 22-12-20017.

CONFLICT OF INTEREST

The authors declare that they have no conflicts of interest.

OPEN ACCESS

This article is licensed under a Creative Commons Attribution 4.0 International License, which permits use, sharing, adaptation, distribution and reproduction in any medium or format, as long as you give appropriate credit to the original author(s) and the source, provide a link to the Creative Commons license, and indicate if changes were made. The images or other third party material in this article are included in the article's Creative Commons license, unless indicated otherwise in a credit line to the material. If material is not included in the article's Creative Commons license and your intended use is not permitted by statutory regulation or exceeds the permitted use, you will need to obtain permission directly from the copyright holder. To view a copy of this license, visit <https://creativecommons.org/licenses/by/4.0/>.

REFERENCES

- Antonova, E.E., Vorobjev, V.G., Kirpichev, I.P., and Yagodkina, O.I., Comparison of the plasma pressure distributions over the equatorial plane and at low altitudes under magnetically quiet conditions, *Geomagn. Aeron. (Engl. Transl.)*, 2014, vol. 54, no. 3, pp. 278–281. <https://doi.org/10.1134/S0016793214030025>
- Antonova, E.E., Kirpichev, I.P., and Stepanova, M.V., Plasma pressure distribution in the surrounding the Earth plasma ring and its role in the magnetospheric dynamics, *J. Atmos. Sol.-Terr. Phys.*, 2014, vol. 115, pp. 32–40. <https://doi.org/10.1016/j.jastp.2013.12.005>
- Antonova, E.E., Stepanova, M., Kirpichev, I.P., et al., Structure of magnetospheric current systems and mapping of high latitude magnetospheric regions to the ionosphere, *J. Atmos. Sol.-Terr. Phys.*, 2018, vol. 177, pp. 103–114. <https://doi.org/10.1016/j.jastp.2017.10.013>
- Baker, K.B. and Wing, S., A new magnetic coordinate system for conjugate studies at high latitudes, *J. Geophys. Res.*, 1989, vol. 94, no. A7, pp. 9139–9144. <https://doi.org/10.1029/JA094iA07p09139>
- Kirpichev, I.P. and Antonova E.E., Plasma pressure distribution in the equatorial plane of the Earth's magnetosphere at geocentric distances of 6–10 R_E according to the international THEMIS mission data, *Geomagn. Aeron. (Engl. Transl.)*, 2011, vol. 51, no. 4, pp. 450–455. <https://doi.org/10.1134/S0016793211040049>
- Kirpichev, I.P., Yagodkina, O.I., Vorobjev, V.G., Antonova, E.E., Position of projections of the nightside auroral oval equatorward and poleward edges in the magnetosphere equatorial plane, *Geomagn. Aeron. (Engl. Transl.)*, 2016, vol. 56, no. 4, pp. 407–414. <https://doi.org/10.1134/S001679321604006X>
- Kirpichev, I.P., Antonova, E.E., Stepanova, M., Eyelade, A.V., Espinoza, C.M., Ovchinnikov, I.L., Vorobjev, V.G., and Yagodkina, O.I., Ion kappa distribution parameters in the magnetosphere of the Earth at geocentric distances smaller than 20 R_E during quiet geomagnetic conditions, *J. Geophys. Res.: Space Phys.*, 2021, vol. 126, e2021JA029409. <https://doi.org/10.1029/2021JA029409>
- Newell, P.T., Feldstein, Ya.I., Galperin, Y.I., and Meng, S.-I., The morphology of nightside precipitation, *J. Geophys. Res.*, 1996, vol. 101, no. A5, pp. 10737–10748. <https://doi.org/10.1029/95JA03516>
- Newell, P.T., Sergeev, V.A., Bikkuzina, G.R., and Wing, S., Characterizing the state of the magnetosphere: testing the ion precipitation maxima latitude (b2i) and the ion isotropy boundary, *J. Geophys. Res.*, 1998, vol. 103, no. A3, pp. 4739–4745. <https://doi.org/10.1029/97JA03622>
- Paschmann, G., Haaland, S., and Treumann, R., Auroral plasma physics, *Space Sci. Rev.*, 2002, vol. 103, pp. 1–485. <https://doi.org/10.1023/A:1023030716698>
- Roach, F.E. and Jannick, P.M., The sky and eye, *Sky Telesc.*, 1958, vol. 17, pp. 164–168.
- Rojas Gamarra, M., Gonzalez, J., Stepanova, M.V., and Antonova, E.E., Variation of plasma pressure at the auroral oval latitudes before, during, and after the isolated geomagnetic substorm on December 22, 2008, *Geomagn. Aeron. (Engl. Transl.)*, 2020, vol. 60, no. 4, pp. 452–460. <https://doi.org/10.1134/S0016793220040131>
- Sergeev, V.A., Malkov, M., and Mursula, K., Testing the isotropic boundary algorithm method to evaluate the magnetic field configuration in the tail, *J. Geophys. Res.*, 1993, vol. 98, no. A5, pp. 7609–7620. <https://doi.org/10.1029/92JA02587>
- Starkov, G.V., Vorobjev, V.G., and Feldstein, Ya.I., Relative position of the regions of auroral precipitation and discrete auroras, *Geomagn. Aeron. (Engl. Transl.)*, 2005, vol. 45, no. 2, pp. 170–180.
- Stepanova, M., Antonova, E.E., and Bosqued, J.-M., Study of plasma pressure distribution in the inner magnetosphere using low-altitude satellites and its importance for the large-scale magnetospheric dynamics, *Adv. Space Res.*, 2006, vol. 38, no. 8, pp. 1631–1636. <https://doi.org/10.1016/j.asr.2006.05.013>
- Tsyganenko, N.A. and Mukai, T., Tail plasma sheet models derived from Geotail particle data, *J. Geophys. Res.*, 2003, vol. 108, no. A3, p. 1136. <https://doi.org/10.1029/2002JA009707>
- Vorobjev, V.G., Kirillov, A.S., Katkalov, Yu.V., and Yagodkina, O.I., Planetary distribution of the intensity of Auroral luminosity obtained using a model of Aurora precipitation, *Geomagn. Aeron. (Engl. Transl.)*, 2013, vol. 53, no. 6, pp. 711–715. <https://doi.org/10.1134/S0016793213060169>
- Vorobjev, V.G., Yagodkina, O.I., and Antonova, E.E., Ion pressure at the auroral precipitation boundaries and its relationship with the solar wind dynamic pressure, *Geomagn. Aeron. (Engl. Transl.)*, 2019, vol. 59, no. 5, pp. 543–553. <https://doi.org/10.1134/S0016793219050141>
- Wing, S. and Newell, P.T., Center plasma sheet ion properties as inferred from ionospheric observations, *J. Geophys. Res.*, 1998, vol. 103, no. A4, pp. 6785–6800. <https://doi.org/10.1029/97JA02994>
- Yahnin, A.G., Sergeev, V.A., Gvozdevsky, B.B., and Vennerstrom, S., Magnetospheric source region of discrete auroras inferred from their relationship with isotropy boundaries of energetic particles, *Ann. Geophys.*, 1997, vol. 15, pp. 943–958. <https://doi.org/10.1007/s00585-997-0943-z>

Translated by M. Chubarova